

# PROCEEDINGS OF SPIE

[SPIDigitalLibrary.org/conference-proceedings-of-spie](https://SPIDigitalLibrary.org/conference-proceedings-of-spie)

## Tomographic imaging of unique objects: annual layers in tooth cementum of Anna Catharina Bischoff born 1719

Jeannette Von Jackowski, Bert Müller, Georg Schulz, Gerhard Hotz, Timm Weitkamp, et al.

Jeannette A. Von Jackowski, Bert Müller, Georg Schulz, Gerhard Hotz, Timm Weitkamp, Ursula Wittwer-Backofen, Christine Tanner, "Tomographic imaging of unique objects: annual layers in tooth cementum of Anna Catharina Bischoff born 1719," Proc. SPIE 12242, Developments in X-Ray Tomography XIV, 122421O (10 November 2022); doi: 10.1117/12.2635312

**SPIE.**

Event: SPIE Optical Engineering + Applications, 2022, San Diego, California, United States

# Tomographic imaging of unique objects: Annual layers in tooth cementum of Anna Catharina Bischoff born 1719

Jeannette A. von Jackowski<sup>\*a,b</sup>, Bert Müller<sup>\*a,b</sup>, Georg Schulz<sup>a,c</sup>, Gerhard Hotz<sup>d,e</sup>, Timm Weitkamp<sup>f</sup>, Ursula Wittwer-Backofen<sup>e</sup>, and Christine Tanner<sup>\*a</sup>

<sup>a</sup>Biomaterials Science Center, Department of Biomedical Engineering, University of Basel, Gewerbestrasse 14, 4123 Allschwil, Switzerland

<sup>b</sup>Biomaterials Science Center, Department of Clinical Research, University Hospital Basel, Schanzenstrasse 55, 4051 Basel, Switzerland

<sup>c</sup>Core Facility Micro- and Nanotomography, Department of Biomedical Engineering, University of Basel, 4123 Allschwil, Switzerland

<sup>d</sup>Natural History Museum of Basel, Anthropological Collection, 4501 Basel, Switzerland

<sup>e</sup>Integrative Prehistory and Archaeological Science, University of Basel, 4055 Basel, Switzerland

<sup>f</sup>Synchrotron SOLEIL, 91190 Saint-Aubin, France

<sup>g</sup>Department of Biological Anthropology, Albert Ludwig University Freiburg, 79110 Freiburg im Breisgau, Germany

## ABSTRACT

The famous Swiss mummy, the "Lady of the Franciscan Church", is located in Basel. Subsequent to discovery in 1975, many investigations of her origin were performed without success. Four decades later, however, the mummy's origin has been identified: Anna Catharina Gernler-Bischoff (1719-1787), who was a direct ancestor of Boris Johnson, the former Prime Minister of the United Kingdom. Further details about her life have been collected. For this purpose, teeth were removed and physically sliced for imaging using optical microscopy. One single tooth remained and became available for this cementochronology study. We have applied microtomography to visualize the annual deposits in tooth cementum, termed incremental layers, without the need of physical slicing. The applicability of synchrotron radiation-based tomography to cementochronology has previously been investigated and showed promise. It is, however, unclear how far tomography will work for the mummy tooth. Laboratory-based microtomography enabled us to discriminate between enamel, dentin, and cementum, but the annual layers remained invisible. The improved density and spatial resolution of the tomography setup at the beamline ANATOMIX, Synchrotron SOLEIL, France, however, brought the incremental layers to light. We have counted 30 layers on average. Their thickness corresponds to  $(4.6 \pm 1.4) \mu\text{m}$ . The available tomography data of the entire tooth should be further analyzed to correlate the life history of Anna Catharina Gernler-Bischoff with thickness and contrast of the incremental layers. The pipeline developed and the gained knowledge will be beneficial for cementochronology of humans dead and alive.

**Keywords:** Mummy, cementochronology, synchrotron radiation-based micro computed tomography, microstructure of archeological teeth, segmentation, incremental layer thickness, tooth cementum thickness, optical microscopy

## 1. INTRODUCTION

In 1975, a mummified female human body was discovered at the Franciscan Church in Basel, Switzerland. This unique object became popular as the "Lady of the Franciscan Church", but her identification took more than four decades, see [https://en.wikipedia.org/wiki/Anna\\_Catharina\\_Bischoff](https://en.wikipedia.org/wiki/Anna_Catharina_Bischoff) [1]. Anna Catharina Gernler-Bischoff was born in March 1719 and died in August 1787, *i.e.* she reached an age of 68 years. During her life, she gave birth to seven children. As a surprise, she was identified as a direct ancestor of Boris Johnson, former Prime Minister of the United Kingdom [2]. Over the years, her life has been reconstructed in more and more detail.

---

\*Send correspondence to J.v.J., e-mail: [jeannette.vonjackowski@unibas.ch](mailto:jeannette.vonjackowski@unibas.ch), B.M., email: [bert.mueller@unibas.ch](mailto:bert.mueller@unibas.ch), C.T., email: [christine.tanner@unibas.ch](mailto:christine.tanner@unibas.ch), [www.bmc.unibas.ch](http://www.bmc.unibas.ch)

Recently, our research team got the opportunity to examine the last preserved tooth of this unique mummy. For this microtomography study, we extracted the remaining tooth of the mummy. Tomography avoids irreversible physical slicing, as required for preparing optical micrographs, so that the tooth could be placed back, as shown in Fig. 1. Figure 1 also displays a series of photographs of the tooth from selected angles of view.



Figure 1. The mummy's tooth remained and a series of four photographs to characterize the tooth morphology from relevant directions, that means buccal, distal, mesial, and lingual. During her lifetime, the woman had lost all the teeth in her upper jaw. Her lower incisors and canines, although decayed, were preserved.

In a first tomography experiment, the entire tooth was made visible by means of a laboratory-based system with the aim to get a reasonable overview of the tooth's geometry/anatomy in the three dimensions with a voxel size of about 10  $\mu\text{m}$ . In a second tomography experiment, we have planned to improve the resolution using a voxel size below one micrometer at the ANATOMIX beamline, Synchrotron Soleil, France. This second experiment should allow us to uncover incremental layers, generally termed annual layers, in the tooth cementum [3].

Because the layers were identified in slices of another tooth of the mummy by optical microscopy, see below, the chance to find them in tomographic data is highly feasible. If the data will allow for the detection of the layers, we might identify characteristics related to the seven childbirths of Anna Catharina Gernler-Bischoff.

There are only a few hard X-ray tomography experiments, which have permitted the explicit imaging of the incremental layers in human tooth cementum with a thickness of three to five micrometers [3-6]. A dataset of an entire human tooth, not yet published, would be a valuable source for quantification, which could include the thickness variation within one layer and between the layers. This information might be meaningfully correlated with stress periods during the life of the selected individual.

## 2. MATERIALS AND METHODS

### 2.1 Two selected teeth of the mummy

The study includes the two canine denoted according to the standard ISO 3950, *i.e.* **23** and **43** both from the "Lady of the Franciscan Church", stored at the Basel Natural History Museum in Switzerland. We professionally extracted the tooth **43**. Subsequently, tooth **43** was placed in an Eppendorf tube for the measurement. After the measurements the tooth was re-implanted. Tooth **23** was removed years ago and sliced. Tooth slices 60 to 80  $\mu\text{m}$ -thin originate from an apical part of the middle third of the tooth root towards the crown.

### 2.2 Tooth cementum analysis using optical microscopy

The single-root tooth **23** served for tooth cementum analysis [7, 8] and was prepared for histology. The optical images of the slices were acquired by means of a Leica DMRXA 2 optical microscope combined with a Leica DC 250 digital camera. The incremental layers were visually identified and manually counted.

### 2.3 Laboratory-based micro computed tomography

The 23 mm-long tooth **43** was imaged using the microtomography system nanotom m<sup>®</sup> (phoenix|x-ray, GE Sensing & Inspection Technologies GmbH, Wunstorf, Germany). It is equipped with a nanofocus transmission target and was operated at an acceleration voltage of 90 kV. The effective pixel length was set to 12  $\mu\text{m}$ . For tomographic imaging, we equiangularly acquired 1,800 radiographs along 360° with an exposure time per radiograph of 12 s.

## 2.4 Synchrotron radiation-based micro computed tomography

Tooth **43** was also imaged at the tomography setup of the ANATOMIX beamline, Synchrotron SOLEIL, France [9]. A white beam was filtered using 20  $\mu\text{m}$ -thin gold and 100  $\mu\text{m}$ -thin copper to obtain a mean photon energy of about 33 keV. During continuous rotation, 9,000 radiographs along 360 degrees were collected with a detection unit consisting of a 20  $\mu\text{m}$ -thin LuAG scintillator coupled to a scientific CMOS-Hamamatsu Orca Flash 4.0 V2-camera with  $2048 \times 2048$  pixels, via a  $10\times$  magnifying lens to reach an effective pixel size of 0.65  $\mu\text{m}$ . The exposure time was set to 100 ms for each radiograph. As the related field-of-view was too small for full-field tomography of the human tooth we have stitched the radiographs in a mosaic fashion on twelve heights [10-12]. Before reconstruction a double flat-field ring-artefact correction and Gaussian filtering with a standard deviation of 0.75 was applied. Tomographic reconstruction was performed with the open-source Python library tomopy, version 1.4.2 [13]. Table 1 lists the image sizes for each of the twelve height steps and the number of stitched field-of-views  $\#R$ .

Table 1. List of the twelve height steps acquired and reconstructed for mummy's tooth **43**, stating the number of recorded rings  $\#R$ , height step position along  $z$ -coordinate, and reconstructed image size in  $x$ - and  $y$ -directions.

Height Step	$\#R$	$z$ [mm]	Image size [pixels]
1	4	40.4	$14,478 \times 10,978$
2	4	41.6	$14,476 \times 10,976$
3	4	42.8	$14,478 \times 10,978$
4	3	44.0	$10,784 \times 7,287$
5	3	45.2	$10,787 \times 7,287$
6	3	46.4	$10,771 \times 7,271$
7	3	47.6	$10,781 \times 7,281$
8	3	48.8	$10,787 \times 7,287$
9	3	50.0	$10,788 \times 7,288$
10	2	51.2	$7,093 \times 3,593$
11	2	52.4	$7,093 \times 3,593$
12	2	53.6	$7,090 \times 3,590$

## 3. RESULTS

### 3.1 Tooth cementum annulation using optical microscopy

Six optical micrographs of slices from canine **23** are represented in Fig. 2. They show the predicted ring-like annual layers to be counted and analyzed. For this purpose, 23 optical micrographs of the ten prepared slices were selected and displayed on a computer screen. By means of the software Imagic IM 1000 from Leica, the contrast was enhanced. For the tooth **23** of the mummy, 41 to 50 layers were identified with a mean value of 44.42. To determine the age-at-death of the mummy, one has to add the formation age of the tooth root. In the case of a female and tooth **23**, one can reasonably assume a formation age of 12.08 years [14]. By adding this value to the mean number of annual layers detected, the tooth cementum analysis method provides an average age-at-death of 56.5 years with a typical error range of  $\pm 2.5$  years.

One can clearly see thickness and contrast variations of the annual layers within the selected optical micrographs represented in Fig. 2. The prominent ones are termed stress bands and originate from a substantial hyper-mineralization, bright layer, and succeeded by a dark layer. Such a feature attracts attention during the manual layer counting and indicate stress conditions during the life of the given individual, which includes pregnancies, renal diseases, and severe skeletal traumata. To systematically identify the stress bands the following procedure had been used. First, by means of three micrographs the average layer thickness and the related standard deviation was determined. Second, the layers that exhibit a thickness corresponding at least to the average value plus one standard deviation have been selected. Third, only if we found these prominent features on two of three micrographs and could assign them to the same layer number, they were

considered as stress bands. For tooth **23** of the mummy, we identified such stress bands for the annual layers #2, #4, #8, #26 and #44.

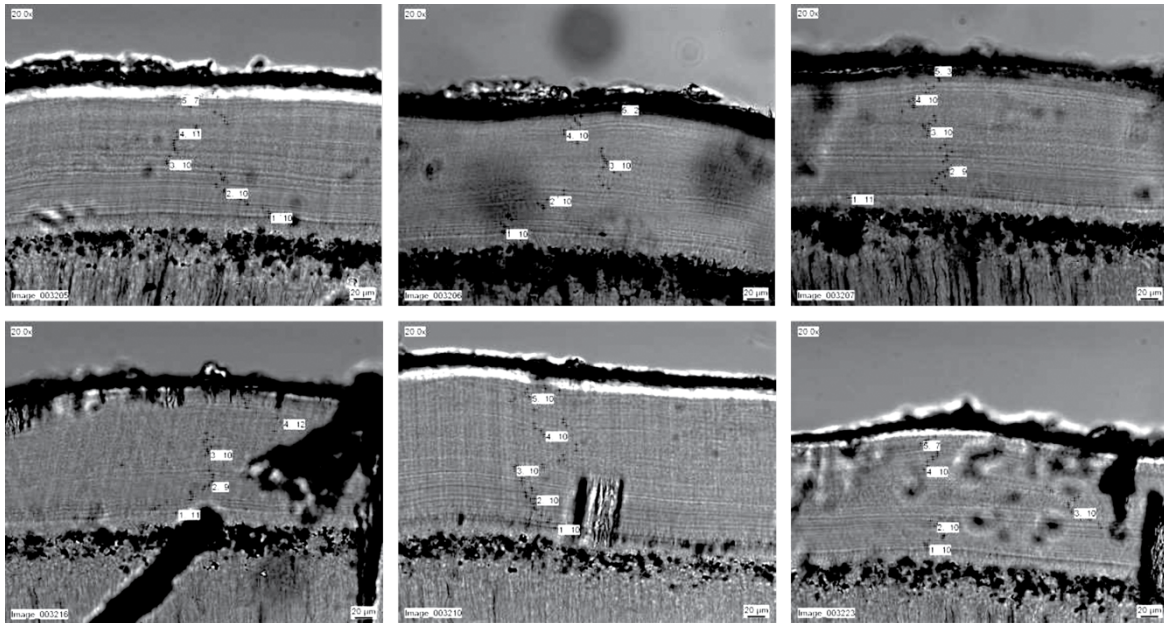


Figure 2. Six selected optical micrographs from slices of canine **23** used to manually annotate and count incremental layers. It is challenging to make the layers simultaneously visible. Therefore, the manual counting is done on a computer screen adapting the contrast for the region of interest. One starts at the cementum-dentin interface and sets labels approximately every ten layers. The results of the counting can vary from region to region, as one can see from the selected micrographs, where in the top row we have identified 48, 42, and 43 layers and the row below 42, 50, and 47 incremental layers.

### 3.2 Conventional microtomography of the canine 43

Laboratory-based microtomography is much easier to access and often provides a larger field-of-view than the setup at a synchrotron radiation facility. Therefore, we performed a tomography measurement of the entire tooth using the nanotom m<sup>®</sup>. This dataset allowed for the visualization of the microanatomy and for the identification of the mineralized tissues, namely enamel, dentin and cementum. It was used to generate the three-dimensional rendering of Fig. 3. The spatial resolution and the contrast, however, were insufficient for the identification of the 2 to 4 µm-thin incremental layers found in the optical micrographs of the slices of canine **23**, cf. micrographs of Fig. 2.

### 3.3 Synchrotron radiation-based microtomography of the canine 43

Synchrotron radiation-based micro computed tomography as performed at the ANATOMIX beamline with a pixel size of 0.65 µm should provide a spatial resolution sufficient for the visualization of the 2 to 4 µm-thin incremental layers of tooth **43** from the mummy. Such an imaging of an entire human tooth, however, is challenging. Because the field-of-view was restricted to (1.3 mm)<sup>2</sup>, stitching of the radiographs with reasonable overlap was necessary. The 9,000 projections along 360° corresponded to angular steps of just 0.04° and might be enough for reconstructing slices with a width of about 15,000 pixels in *x*- and *y*-directions. To image the part of interest from the entire tooth in *z*-direction, twelve height steps were necessary.

Compared to the tooth slices used for optical microscopy with a thickness of 60 to 80 µm, the virtual slices are about two orders of magnitude thinner. Thus, a direct comparison might be improper. As a consequence, we decided to generate projections of 55 virtual slices, as represented in Fig. 4 for the central part of each of the twelve height steps. The images of the 12 virtual slices give the reader an idea on the maximal tooth diameter for each height step and the required number of rings #*R* listed in the second column of Table 1.

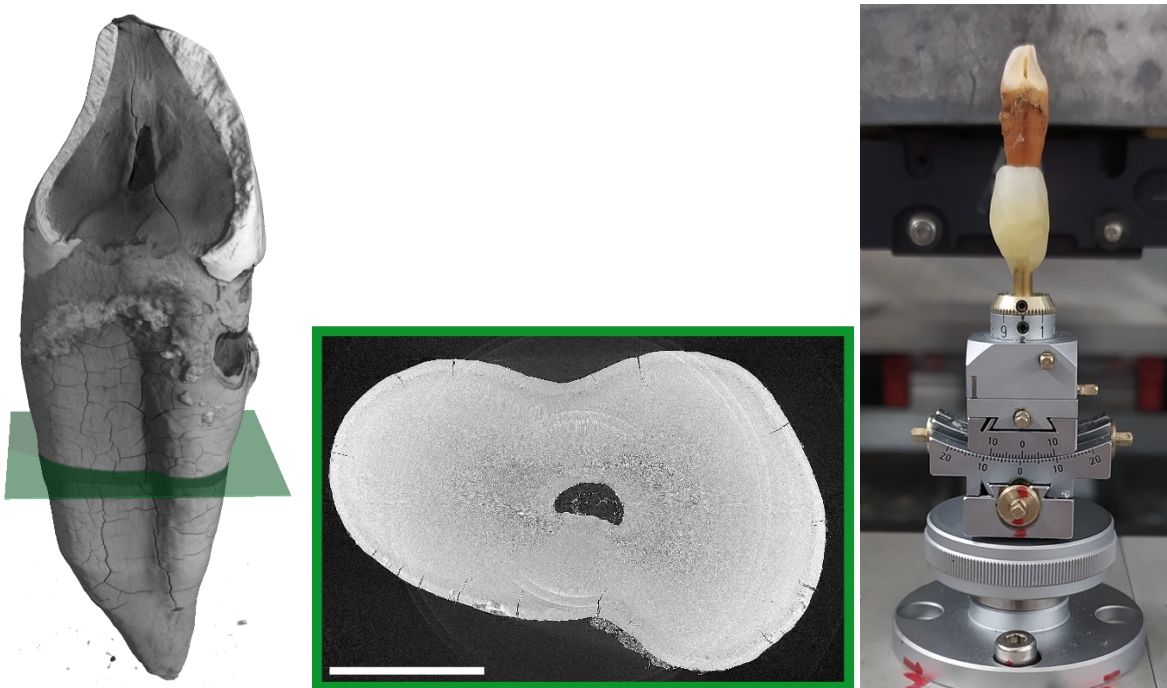


Figure 3. Three-dimensional rendering of mummy's tooth 43 based on nanotom m<sup>®</sup> data. The green-colored plane corresponds to the position of the virtual slice represented in the center of the figure. This slice from Height Step #5 was acquired at the ANATOMIX beamline, Synchrotron SOLEIL, France. One can not only see the dentin with the cementum at the periphery, but also the cracks formed. The length bar corresponds to 2 mm. For the data acquisition at the synchrotron radiation facility, the unique tooth was fixed on the holder of the precision manipulator by means of wax, as shown on the right of the figure.

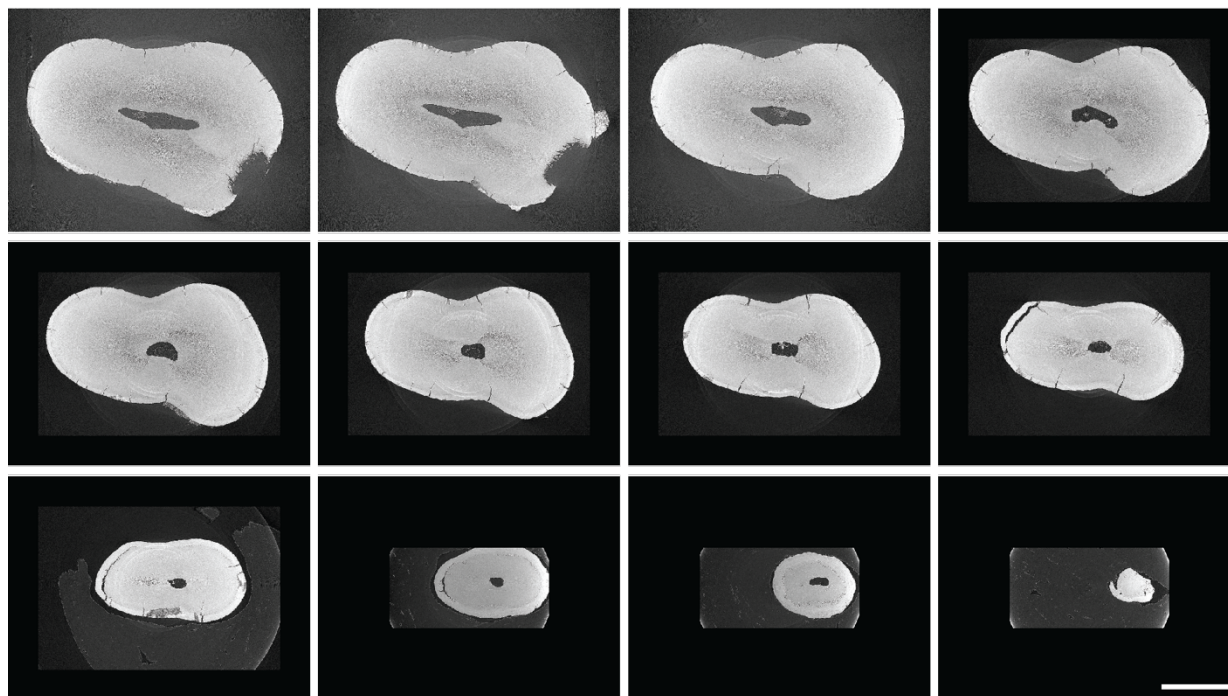


Figure 4. Mean projection of 55 slices corresponding to a thickness of 35  $\mu\text{m}$  from the center of each of the twelve height steps, data acquired at the ANATOMIX beamline, Synchrotron SOLEIL, France. Gray-scale intensity is scaled from second to 98th percentile. The length bar corresponds to 2 mm.

The slices shown in Figs. 3 and 4 allow for the manual cementum segmentation. The incremental layers, however, are hardly ever detectable. Therefore, we followed our previous approach [15], which is explained in Fig. 5, with the aim to optimize integration along the incremental layer direction. After the manual segmentation of the cementum, blue colored, the sections were straightened. Thereafter, the integration direction was automatically optimized section-by-section. The integration over 55 slices, *i.e.* along 35  $\mu\text{m}$ , yielded the enhanced image for annual layer identification, cf. Figs. 5 and 6.

The four regions selected for incremental layer identification are shown Fig. 6. The layers are clearly visible and marked by yellow-colored plus signs on the basis of visual inspection. Their structure resembles the annual layers of tooth 23 displayed by the optical micrographs in Fig. 2.

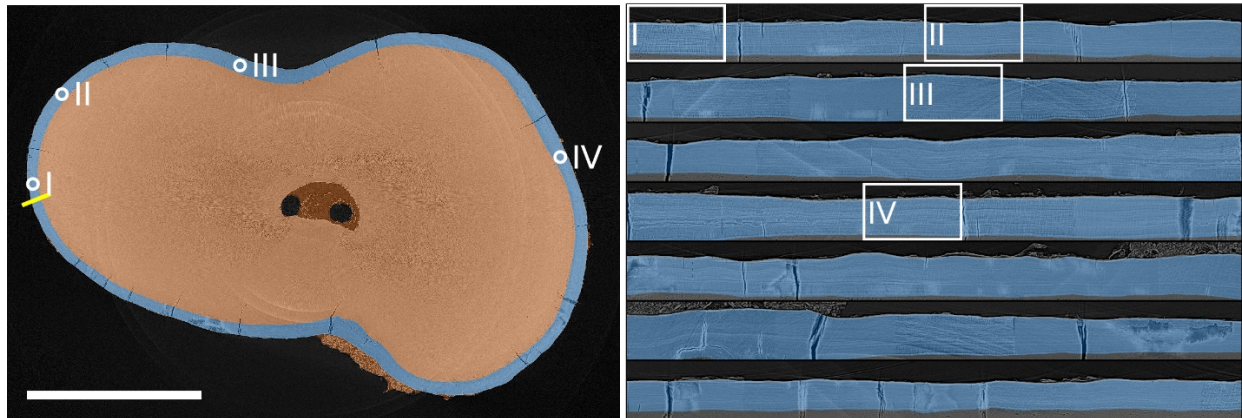


Figure 5. Cross section of Height Step #5 with tooth cementum segmented and represented using blue color. On the right, the cementum is straightened and given from the yellow marker in clock-wise sampling. The framed regions I to IV are used for annotations, see below, and their center locations are shown by the white circles in the selected virtual slice. The length bar is 2 mm long.

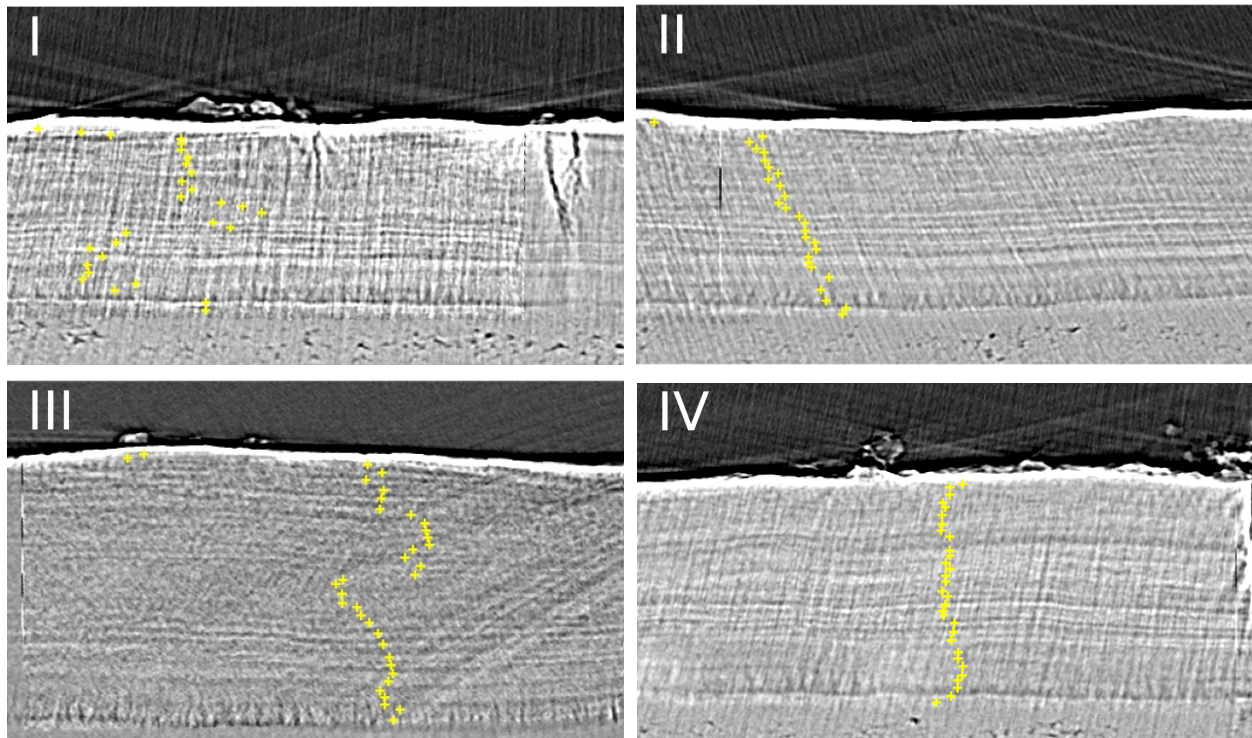


Figure 6. Manually annotated incremental layers, cf. yellow plus signs, for the user-selected regions I to IV from Fig. 5.

The images of Fig. 6 show clearly demarcated layers often better identifiable than in the optical micrographs, cf. Fig. 2. The number of layers for tooth **43** were between 27 and 35, which is substantially lower than found via optical micrographs of tooth **23** from the same individual. Table 2 does not only list the number of incremental layers but also their thickness. The mean thickness value of the incremental layers is  $(4.6 \pm 1.5) \mu\text{m}$ . Within the standard deviation the value corresponds to the ones from optical micrographs with a strong tendency to thicker layers.

Starting from the dentin-cement interface, the incremental layers show a characteristic behavior, found in the regions investigated without exception. The first third of the cementum contains well-visible layers irregular in appearance and spacing. In the second third, we observed prominent and regular layers. The layers of the last third are regular but weak in contrast.

Table 2. Quantification of the incremental layers in tooth cementum: For each of the four regions marked in Fig. 6, the number of the bright incremental layers #ILs were manually counted. The individual distances of the incremental layers and the acellular extrinsic fiber cementum thickness are listed.

Region	#ILs	Distance of ILs [ $\mu\text{m}$ ]					Cementum thickness [ $\mu\text{m}$ ]	
		mean	std	min	median	max	ILs	local
I	28	4.2	1.4	2.0	4.1	7.9	114.8	120.9
II	27	4.7	1.5	2.3	4.4	9.1	121.5	125.5
III	35	4.9	1.3	2.6	4.9	8.1	168.2	181.3
IV	31	4.6	1.4	2.0	4.5	8.7	138.0	143.0
Mean	30	4.6	1.4	2.3	4.5	8.5	135.6	142.7

## 4. DISCUSSION

Tooth cementum is an avascular tissue that anchors tooth roots by mineralizing collagen fiber bundles [16]. Cementum is continuously deposited and grows in layers. They were made visible in cross-sections through tooth roots using optical and electron microscopies [17]. These measurements demonstrated that the crystalline orientation and their size could be responsible for the layered appearance of cementum. Therefore, it has not been a surprise that they also became visible in phase-contrast mode tomography [6]. It is important to mention that not only tomography setups at synchrotron radiation facilities can be used to visualize the incremental layers in human tooth cementum, but advanced laboratory-based tomography systems also allow for their identification [18].

### 4.1 Tooth cementum annulation

Tooth cementum annulation using optical microscopy often underestimates the age-at-death – especially for ages above 50 years [19-22]. This observation is also valid for the present study. The estimated age-at-death is 56.5 years and even if we consider the error of 2.5 years, the age-at-death derived from the cementum annulation of tooth **23** is underestimated by more than eight years. Also the maximally found number of layers of 50 cannot explain the age-at-death of Anna Catharina Gernler-Bischoff.

The number of layers identified within the four selected regions of the tomography data from tooth **43** ranged from 27 to 35. Taking into account the maximal number and considering the maximal eruption age of tooth **43** of 14.5 years [14], one finds an age-at-death of 49.5 years. This age is much less than the documented age-at-death of Anna Catharina Gernler-Bischoff.

We can only speculate on the discrepancies between the number of counted layers in tooth cementum and the documented age-at-death. First, the variation of counted layers from region to region may indicate that some of the annual layers are interrupted along the circumference. Second, the outer part of the cementum might have unintentionally been removed implying less layers could be counted. A visual inspection of the tooth, cf. Fig. 1, verifies that the part of interest is well preserved. Third, the spatial and density resolution of both optical microscopy and hard X-ray tomography might be insufficient to identify the thinnest layers, *i.e.* layers with a thickness below  $2 \mu\text{m}$ . Since the spatial resolution of the optical microscopy is probably slightly better than the one of the microtomography, we can explain the higher number of

detected layers using optical microscopy, although the teeth originate from different positions. This assumption is also in agreement with a recently performed comparative study [15].

#### 4.2 Irregularities in layer width and appearance

Irregular layers in the tooth cementum have been associated with stress conditions, for example as a result of disease and pregnancy [23]. Kagerer and Grupe [21] demonstrated that especially pregnancies, skeletal traumata and renal diseases have a marked influence on the calcium metabolism resulting in prominent incremental layers. Unfortunately, the medical history of the mummy is unknown; several diseases including atherosclerosis, syphilis, and gallstones are highly probable. The childbirths of Anna Catharina Gernler-Bischoff, however, were documented. Her children were christened on the following dates: November 27, 1738 (Theodor Gernler), November 27, 1739 (Anna Catharina Gernler), May 11, 1741 (Valeria Gernler), February 27, 1744 (Augusta Maria Gernler), April 2, 1746 (Salome Gernler), October 8, 1749 (Lukas Gernler), and November 25, 1751 (Johann Lukas Gernler). This means that Anna Catharina Gernler-Bischoff gave births at the ages of 19.7, 20.7, 22.1, 24.9, 27.0, 30.5, and 32.7 years. These timepoints do not coincide with the stress bands found by means of optical microscopy.

As prominent annual layers are present in the tomography data of middle third of the tooth cementum, which corresponds to the reproductive age of Anna Catharina Gernler-Bischoff, a correlation with the known childbirths makes sense. Therefore, we tried to correlate this pattern with the annual layers identified by microtomography. For this purpose, we assumed an eruption age of tooth 43 of 14.5 years and started the counting at the dentin-cementum interface. The layers marked in the selected regions of Figure 7 are hardly dominant. Nonetheless, an interrelation between childbirths and pronounced appearance cannot be excluded. The analysis of Mani-Caplazi *et al.* [23] proved the challenges in the identification of pregnancies from the appearance and width of incremental layers.

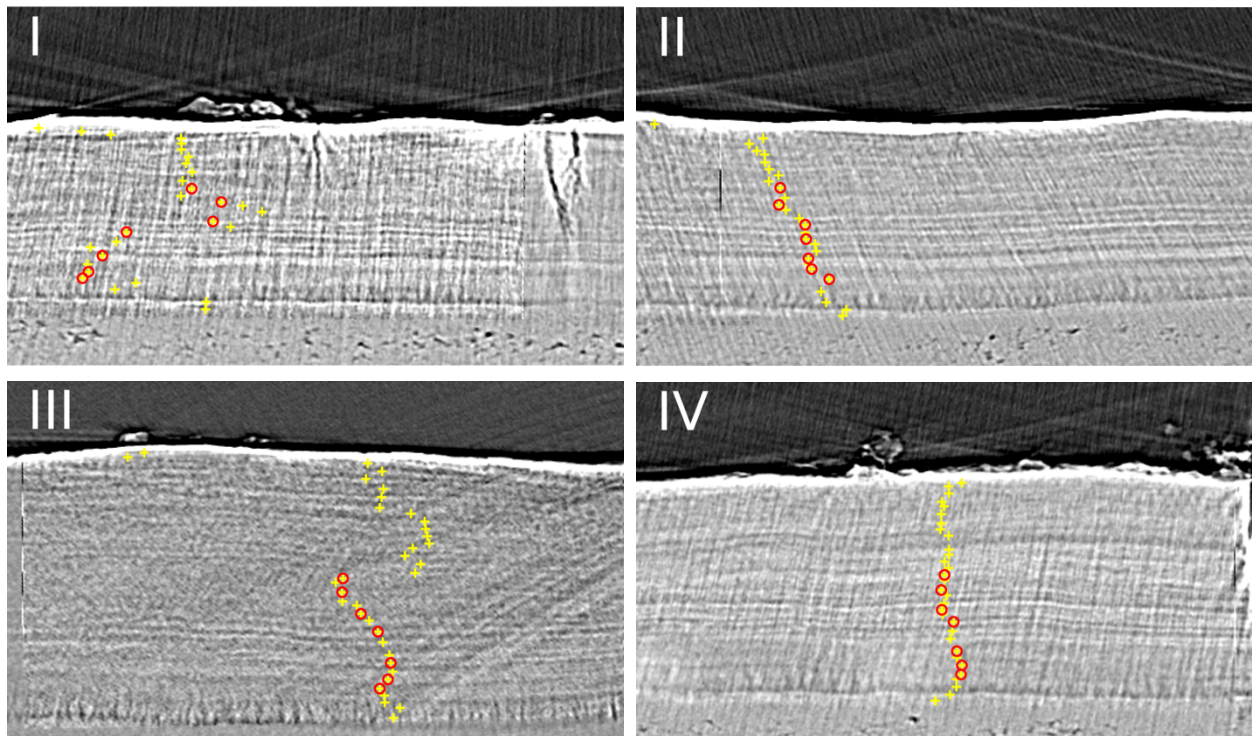


Figure 7. The annotated incremental layers marked by the yellow plus signs are shown together with the presumed layer growth at childbirths marked by the red circles.

#### 4.3 Suggestions for more detailed tomography-based research on the mummy's tooth cementum

The analysis of the incremental layers of the tooth cementum is restricted on rather small regions, although the tomography data of the entire cementum of interest are available. The analysis of the entire dataset could be used to determine potential

interruptions of individual layers along the circumference. It could also allow for the determination of the layer thickness variations along one layer and between the layers, provided that the challenging segmentation will be successful. Such an analysis would also allow determining the locations of well-distinguishable layers.

Using a pixel length of 0.65  $\mu\text{m}$ , incremental layers with a thickness below 2  $\mu\text{m}$  are generally invisible. Therefore, future tomography measurements should be carried out with a better spatial resolution presumably using a moderate magnification by X-ray optics.

## 5. CONCLUSION

Microtomography is a powerful tool to investigate calcified tissues including human teeth. In a tooth of a known mummy, the cementum can be easily identified, even if laboratory-based instruments are employed. The annotation of dozen of incremental layers, which are generally termed annual rings, however, requires the application of state-of-the-art computational tools on tomography data specially recorded at a synchrotron radiation facility.

## ACKNOWLEDGEMENTS

The authors are thankful to Marina Zulauf, Basel, Switzerland, for identifying the documented dates of christening of the seven children of Anna Catharina Gernler-Bischoff. The financial support of the Swiss National Science Foundation within the project No. 133802 is gratefully acknowledged. Beamtime at the ANATOMIX beamline was granted by Synchrotron SOLEIL under proposal 20200712. ANATOMIX is an Equipment of Excellence (EQUIPEX) funded by the Investments for the Future program of the French National Research Agency (ANR), project NanoimagesX, grant no. ANR-11-EQPX-0031.

## REFERENCES

- [1] Grahan, J. A., [Anna Catharina Bischoff] Wikipedia, (2022).
- [2] Foulkes, I., [Boris Johnson 'is descendant' of mummified Basel woman], (2018).
- [3] Naji, S., Rendu, W., and Gourichon, L., [Dental Cementum in Anthropology] Cambridge University Press, Cambridge, (2022).
- [4] Cerrito, P., Nava, A., Radovčić, D., Borić, D., Cerrito, L., Basdeo, T., Ruggiero, G., Frayer, D. W., Kao, A. P., Bondioli, L., Mancini, L., and Bromage, T. G., "Dental cementum virtual histology of Neanderthal teeth from Krapina (Croatia, 130-120 kyr): an informed estimate of age, sex and adult stressors," *Journal of the Royal Society Interface* **19**(187), 20210820 (2022).
- [5] Le Cabec, A., Tang, N. K., Ruano Rubio, V., and Hillson, S., "Nondestructive adult age at death estimation: Visualizing cementum annulations in a known age historical human assemblage using synchrotron X-ray microtomography," *American Journal of Physical Anthropology* **168**(1), 25-44 (2019).
- [6] Mani-Caplazi, G., Schulz, G., Deyhle, H., Hotz, G., Vach, W., Wittwer-Backofen, U., and Müller, B., "Imaging of the human tooth cementum ultrastructure of archeological teeth, using hard X-ray microtomography to determine age-at-death and stress periods," *Proc. SPIE* **10391**, 103911C (2017).
- [7] Perrone, V., Gocha, T. P., Randolph-Quinney, P., and Procopio, N., "Tooth cementum annulation: A literature review," *Forensic Sciences* **2**(3), 516-550 (2022).
- [8] Wittwer-Backofen, U., "Age estimation using tooth cementum annulation," *Methods in Molecular Biology* **915**, 129-43 (2012).
- [9] Weitkamp, T., Scheel, M., Giorgetta, J. L., Joyet, V., Le Roux, V., Cauchon, G., Moreno, T., Polack, F., Thompson, A., and Samama, J. P., "The tomography beamline ANATOMIX at Synchrotron SOLEIL," *Journal of Physics: Conference Series* **849**(1), 012037 (2017).
- [10] Rodgers, G., Tanner, C., Schulz, G., Weitkamp, T., Scheel, M., Girona Alarcón, M., Kurtcuoglu, V., and Müller, B., "Mosaic microtomography of a full mouse brain with sub-micron pixel size," *Proc. SPIE* **12242**, 122421L (2022).

- [11] Tanner, C., Müller, B., and Rodgers, G., "Registration of microtomography images: Challenges and approaches," *Proc. SPIE* **12242**, 122420T (2022).
- [12] Tanner, C., Rodgers, G., Schulz, G., Osterwalder, M., Mani-Caplazi, G., Hotz, G., Scheel, M., Weitkamp, T., and Müller, B., "Extended-field synchrotron microtomography for non-destructive analysis of incremental lines in archeological human teeth cementum," *Proc. SPIE* **11840**, 1184019 (2021).
- [13] Gürsoy, D., De Carlo, F., Xiao, X., and Jacobsen, C., "TomoPy: a framework for the analysis of synchrotron tomographic data," *Journal of Synchrotron Radiation* **21**(Pt 5), 1188-93 (2014).
- [14] Khan, A. S., Nagar, P., Singh, P., and Bharti, M., "Changes in the sequence of eruption of permanent teeth; Correlation between chronological and dental age and effects of body mass index of 5-15-year-old schoolchildren," *International Journal of Clinical Pediatric Dentistry* **13**(4), 368-380 (2020).
- [15] Müller, B., Stiefel, M., Rodgers, G., Humbel, M., Osterwalder, M., von Jackowski, J. A., Hotz, G., Velasco Guadarrama, A. A., Bunn, H. T., Scheel, M., Weitkamp, T., Schulz, G., and Tanner, C., "Three-dimensional imaging and analysis of annual layers in tree trunk and tooth cementum," *Proc. SPIE* **12041**, 120410C (2022).
- [16] Lieberman, D. E., "Life history variables preserved in dental cementum microstructure," *Science* **261**(5125), 1162-4 (1993).
- [17] Cool, S. M., Forwood, M. R., Campbell, P., and Bennett, M. B., "Comparisons between bone and cementum compositions and the possible basis for their layered appearances," *Bone* **30**(2), 386-92 (2002).
- [18] Migga, A., Schulz, G., Rodgers, G., Osterwalder, M., Tanner, C., Blank, H., Jerjen, I., Salmon, P., Twengström, W., Scheel, M., Weitkamp, T., Schlepütz, C. M., Bolten, J. S., Huwyler, J., Hotz, G., Madduri, S., and Müller, B., "Comparative hard x-ray tomography for virtual histology of zebrafish larva, human tooth cementum, and porcine nerve," *Journal of Medical Imaging* **9**(3), 031507 (2022).
- [19] Bertrand, B., Cunha, E., Bécart, A., Gosset, D., and Hédouin, V., "Age at death estimation by cementochronology: Too precise to be true or too precise to be accurate?," *American Journal of Physical Anthropology* **169**(3), 464-481 (2019).
- [20] Dias, P. E., Beaini, T. L., and Melani, R. F., "Age estimation from dental cementum incremental lines and periodontal disease," *Journal of Forensic Odontostomatology* **28**(1), 13-21 (2010).
- [21] Kagerer, P., and Grupe, G., "Age-at-death diagnosis and determination of life-history parameters by incremental lines in human dental cementum as an identification aid," *Forensic Science International* **118**(1), 75-82 (2001).
- [22] Naji, S., Colard, T., Blondiaux, J., Bertrand, B., d'Incau, E., and Bocquet-Appel, J. P., "Cementochronology, to cut or not to cut?," *International Journal of Paleopathology* **15**, 113-119 (2016).
- [23] Mani-Caplazi, G., Hotz, G., Wittwer-Backofen, U., and Vach, W., "Measuring incremental line width and appearance in the tooth cementum of recent and archaeological human teeth to identify irregularities: First insights using a standardized protocol," *International Journal of Paleopathology* **27**, 24-37 (2019).